Journal of Engineering Mathematics **45:** 379–399, 2003.

Intermediate asymptotics for Richards' equation in a finite layer

THOMAS P. WITELSKI
Duke University, Department of Mathematics, Durham, North Carolina, 27708-0320, U.S.A.

Received 25 November 2001; accepted in revised form 29 August 2002

Abstract. Perturbation methods are applied to study an initial-boundary-value problem for Richards' equation, describing vertical infiltration of water into a finite layer of soil. This problem for the degenerate diffusion equation with convection and Dirichlet/Robin boundary conditions exhibits several different regimes of behavior. Boundary-layer analysis and short-time asymptotics are used to describe the structure of similarity solutions, traveling waves, and other solution states and the transitions connecting these different intermediate asymptotic regimes.

Key words: groundwater flow, intermediate asymptotics, nonlinear diffusion, perturbation expansions

1. Introduction

In this article, we use an array of asymptotic techniques to give a complete description of the behavior in a mathematical model for the vertical infiltration of rainwater into a finite layer of dry soil. This is a problem of great practical interest in the study of fluid flow in porous media [1, Chapter 9], [2–5]. Our model for this problem is a special case of Richards' equation [6] for the transport of water content $u = u(x, t)$ in unsaturated soil, with the position x being measured downward into the soil layer,

$$\frac{\partial u}{\partial t} + \frac{\partial (u^k)}{\partial x} = \frac{\partial^2 (u^k)}{\partial x^2}. \tag{1.1}$$

The dynamics of this equation have been studied extensively for the Cauchy problem describing the transport of a finite release of a contaminant [7–9].

Interestingly, the solution of the initial-boundary-value problem for (1.1) for the infiltration of water from a steady source into a finite soil layer with an impervious lower boundary exhibits several different stages of behavior. As shown in Figures 1 and 2, for short times there is a transient regime described by a similarity solution before the flow develops into a steady traveling-wave profile. Later, the flow reaches the impervious boundary and water begins to accumulate at the base of the soil layer. Subsequently, depending on conditions, the soil at the base of the layer can saturate with water, yielding a saturation wave that propagates upward through the layer, or if saturation does not occur, then a slower diffusive wave transports water upward through the layer. This is a surprisingly rich set of dynamics for Equation (1.1); it includes several transitions between different regimes of behavior. This problem can serve to provide more insight into new problems for flow in layered soils [10], and problems for more sophisticated models [11, 12]. Moreover, the asymptotic formulae derived here give nearly complete information about the key aspects of the flow for all times, $0 \leq t < \infty$. This defers the need for numerical simulations [13] of this fundamental problem. The solutions presented here certainly do not eliminate the pressing need for numerical calculations of flows in porous

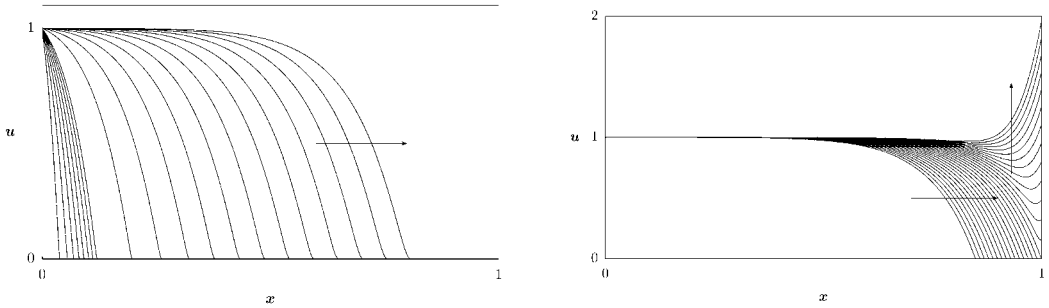

Figure 1. (left) The starting flow regime – initial transient behavior and the convergence to a traveling wave. (right) Stopping behavior as the traveling wave runs into the impermeable boundary at $x = 1$ and leads to the accumulation of water at the boundary.

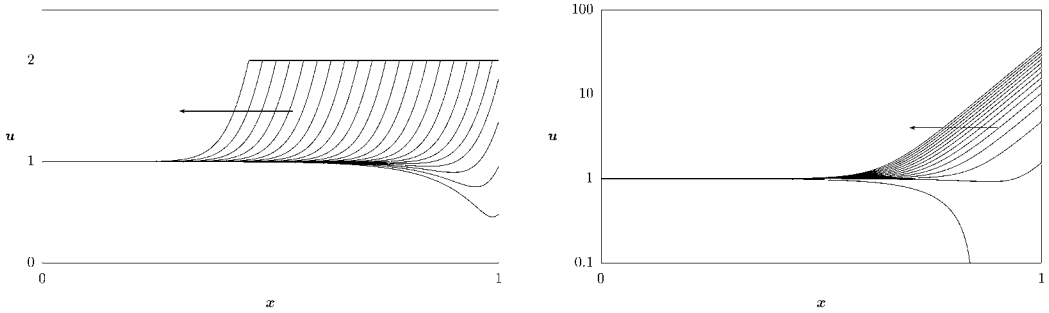

Figure 2. The reverse flow regime – for longer times, the flow is dominated by the no-flux boundary condition: (left) with saturation there is a well-defined saturation front, (right) diffusive reverse flow without saturation.

media, but they do provide an analytical starting point which may make computations of much more challenging problems more tractable.

In addition to the role of (1.1) as Richards' equation for fluid flow in porous media, this problem is of interest in many other settings. Equation (1.1) is a generalized Burgers' equation and has been studied in connection with nonlinear diffusive waves [14, Chapter 4], [15, 16]. A very similar equation also describes the basic lubrication model for the free-surface flow of thin viscous films driven by gravity [17]. Furthermore, in absence of the convective term, for $k > 1$ Equation (1.1) is a nonlinear degenerate diffusion equation called the porous-medium equation. This model has attracted enormous mathematical attention for its special properties [18, 19], [20, Chapter 2] and its applications to modeling other physical systems [21, 22].

In many ways, this article serves to continue the use of asymptotic techniques to describe flow in porous media begun in [23, 24]. There, attention was focused on the leading-order analysis of the interaction of the flow with a boundary. Here, that 'stopping behavior' is extended to higher order and it is only one of several regimes that go into constructing the overall description of the dynamics. Indeed, many classes of *intermediate asymptotic* regimes, as described in [20, Chapter 2], are exhibited by the boundary-value problem we consider. We combine known results on the early stages of the dynamics with new results derived for the later stages to yield this overall description of the problem.

The existence of these different regimes of behavior provides insight into changes in the dominant mechanisms controlling different stages of the flow. For short-times, this is represented by a transition from a diffusive similarity solution [22] to a traveling wave solution [14, Chapter 4]; this is called the starting flow and is described in Section 4. For longer times,

the influence controlling the dynamics changes from the boundary condition at the surface of the layer to the boundary condition at the base of the layer, see Section 5. This transition is accompanied by the destabilization of the in-flow traveling wave in favor of reverse flow, given by either a traveling wave, see Section 6, or a diffusive solution, see Section 7.

On first sight (1.1) does not contain an obvious small parameter for use in asymptotic analysis of the problem. However, through the use of mathematical properties of degenerate diffusion equations and classical perturbation methods including multiple scale analysis, boundary layers, and artificial small parameters [25, Chapter 3], we will solve an array of problems that will cumulatively give us a very good approximation of the full dynamics of our problem for (1.1).

2. Formulation

Beginning in dimensional form, we examine the problem for Richards' equation [6] for the vertical transport of water into a finite layer of homogeneous soil,

$$\frac{\partial U}{\partial T} + \frac{\partial}{\partial X}\left(K(U)\right) = \frac{\partial}{\partial X}\left(D(U)\frac{\partial U}{\partial X}\right), \qquad 0 \le X \le L, \tag{2.1}$$

where $U(X, T) \ge 0$ is the local moisture content, X represents a position measured downward into the soil layer, and $K(U)$ and $D(U)$ describe the hydraulic conductivity and diffusivity of the soil respectively [1, Chapter 9], [26, Chapter 3]. We assume that the layer is initially dry at time $T = 0$,

$$U(X, 0) = 0. \tag{2.2}$$

For $X > L$, we imagine that the deeper layers of soil are either of a coarser grade, or entirely impermeable. Hence, we impose a no-flux condition at the boundary,

$$\left.\frac{\partial U}{\partial X}\right|_{X=L} = \frac{K(U)}{D(U)}. \tag{2.3}$$

If the soil is of a coarser grade for $X > L$, then the moisture will not be able to propagate past $X = L$ until a minimum entry pressure has been achieved at the stratification surface; we will neglect this possibility and strictly enforce (2.3). At the surface of the layer, we assume that there is a steady source of water,

$$U(0, T) = U_0. \tag{2.4}$$

We will focus on the solution of this problem for Brooks-Corey soils [26, Chapter 3] with conductivity and diffusivity taken to be of the forms

$$K(U) = K_0 U^k, \qquad D(U) = D_0 U^n, \tag{2.5}$$

with $k \ge 1, n \ge 0$. Further, we will restrict our presentation to the case where $k = n + 1$, where a closed-form traveling-wave solution can be found [24]. However, more generally, our results can be extended to other soil models that have the same limiting behavior (2.5) for $U \to 0$.

To complete the statement of the problem, we must acknowledge that soils can become saturated at a finite level of moisture content, $U = U_s$. Richards' equation (2.1) describes the flow in unsaturated regions of the soil layer, where $U < U_s$. For this vertical infiltration problem, the solution, taking account of the possibility of saturation, will be of the form

$$U(X,T) = \begin{cases} \text{solution of (2.1)} & 0 \le X \le X_s(T), \\ U_s & X_s(T) \le X \le L, \end{cases} \tag{2.6}$$

where $X_s(T)$ is the position of the saturation interface. If the entire layer is unsaturated, then we define $X_s = L$. At $X_s(T)$, we impose a no-flux condition like (2.3) since there can be no further flux into the already saturated soil.

Applying our assumptions for the soil model reduces (2.1) to

$$\frac{\partial U}{\partial T} + K_0 \frac{\partial}{\partial X}\left(U^{n+1}\right) = D_0 \frac{\partial}{\partial X}\left(U^n \frac{\partial U}{\partial X}\right), \tag{2.7}$$

with linear boundary condition, at the impervious boundary at $X = L$,

$$D_0 \frac{\partial U}{\partial X}\bigg|_{X=L} = K_0 U(L,T). \tag{2.8}$$

We can non-dimensionalize this problem using the scalings

$$U = U_0 u, \qquad X = Lx, \qquad T = \tau t. \tag{2.9}$$

Balancing the time derivative with the convective terms yields the time-scale

$$\tau = \frac{L}{K_0 U_0^n}. \tag{2.10}$$

The contribution of the diffusivity is scaled by the reciprocal of the Peclet number,

$$\text{Pe} = \frac{K_0 L}{D_0}. \tag{2.11}$$

The nondimensionalized problem for the unsaturated flow is then

$$\frac{\partial u}{\partial t} + \frac{\partial}{\partial x}\left(u^{n+1}\right) = \frac{1}{\text{Pe}} \frac{\partial}{\partial x}\left(u^n \frac{\partial u}{\partial x}\right), \qquad 0 \le x \le 1, \tag{2.12}$$

with boundary conditions

$$u(0,t) = 1, \qquad \frac{1}{\text{Pe}} \frac{\partial u}{\partial x}\bigg|_{x=1} = u(1,t), \tag{2.13}$$

and initial condition

$$u(x,0) = 0. \tag{2.14}$$

Equation (2.12) is a degenerate parabolic equation; it is well known that it supports non-negative weak solutions that have a discontinuous derivative at the wetting interface $x_w(t)$ (or edge of support) where the solution vanishes, $u(x_w(t),t) = 0$. These solutions have finite speed of propagation of the interface [18, 27], a mathematical property that makes this class of model equations seem more physically appropriate for many transport problems [28]. Local analysis of (2.12) with the imposition of the condition that there is no unphysical flux into the dry region ahead of the interface position yields an equation for the motion of the wetting interface,

$$\frac{\mathrm{d}x_w}{\mathrm{d}t} = -\frac{1}{\text{Pe}} u^{n-1} \frac{\partial u}{\partial x}\bigg|_{x \to x_w^-}, \qquad u(x \to x_w) = 0. \tag{2.15}$$

From the scalings (2.9), if the soil has a sufficiently low saturation level then we will have to impose the extra condition on the flow, that

$$u(x,t) \le u_s \qquad \text{with} \qquad u_s \equiv \frac{U_s}{U_0} > 1. \tag{2.16}$$

While the solution is uniformly less than u_s this condition does not come into effect. However, because of the accumulation of moisture at the impervious boundary, for longer times, the maximum of the solution will grow in a monotone manner until it reaches the equilibrium solution of (2.12, 2.13), $\bar{u}(x) = \mathrm{e}^{\mathrm{Pe}x}$, or it reaches the saturation level u_s. If $u_s < \mathrm{e}^{\mathrm{Pe}}$, then eventually there will be a finite portion of the layer, $x_s \le x \le 1$, where the soil is saturated with water and the solution there is $u(x,t) \equiv u_s$. There will be a moving interface, $x_s(t)$, separating regions of saturated and unsaturated soil. At the saturation interface, there can be no further flux of moisture into the saturated region, hence we impose the no-flux boundary conditions at the moving boundary,

$$u(x_s(t),t) = u_s, \qquad \frac{1}{\mathrm{Pe}}\frac{\partial u}{\partial x}\bigg|_{x\to x_s^-} = u_s, \tag{2.17}$$

and the domain where Richards' equation (2.12) is applied just to the unsaturated zone, $0 \le x \le x_s(t)$. From physical considerations, it is clear that the saturated zone will grow steadily, with $x_s(t)$ monotone decreasing until it approaches its positive steady-state value, $\bar{x}_s = \log(u_s)/\mathrm{Pe}$.

3. Traveling-wave solutions

As we will see, for several regimes in our problem, the asymptotic solution is given by a traveling wave, so before proceeding, we briefly summarize the results for these wave solutions.

A traveling wave of (2.12) is found by assuming a solution of the form $u(x,t) = \mathcal{U}(x-ct)$ where c is the propagation speed. This *ansatz* reduces Richards' equation to the ordinary differential equation

$$-c\frac{\mathrm{d}\mathcal{U}}{\mathrm{d}\xi} + \frac{\mathrm{d}}{\mathrm{d}\xi}\left(\mathcal{U}^k\right) = \frac{1}{\mathrm{Pe}}\frac{\mathrm{d}}{\mathrm{d}\xi}\left(\mathcal{U}^n\frac{\mathrm{d}\mathcal{U}}{\mathrm{d}\xi}\right), \tag{3.1}$$

where $\xi = x - ct$. For appropriate conditions on (k,n), there will be steady-profile, front-type solutions of this equation [14, Chapter 4]. In the context of the current problem, we integrate (3.1) and apply the boundary conditions of a constant source $u = 1$ and the interface condition at the leading edge of the traveling wave (2.15). This yields that the velocity is $c = 1$, hence our choice for the normalization of u has also given us traveling-wave dynamics with an $O(1)$ time-scale. The solution can then be written in implicit form as

$$\xi = \frac{1}{\mathrm{Pe}}\int_0^{\mathcal{U}} \frac{U^n\,\mathrm{d}U}{U^k - U}, \tag{3.2}$$

where the wetting front is specified to be at $\xi = 0$. This traveling wave solution is commonly called the 'profile at infinity' in the literature on flow in porous media [29–32].

The solution (3.2) describes the flow for $\xi \le 0$; for $\xi > 0$ the solution is $\mathcal{U} \equiv 0$. The fact that there is a well-defined position of the wetting interface is a well-known result of nonlinear degenerate diffusion [18, 27, 28]. For convenience, we restrict our presentation to the case $k = n + 1$ where (3.2) yields the closed-form solution for any positive $n > 0$,

$$\mathcal{U}_0(\xi) = \left(1 - \mathrm{e}^{n\mathrm{Pe}\xi}\right)_+^{1/n}, \tag{3.3}$$

where we introduce the notation for the non-negative truncated weak solution: $v_+ \equiv \max(v, 0)$. The subscript zero indicates that this traveling wave is compactly supported and is propagating into dry soil with $u \equiv 0$. The techniques applied in the following sections can still be used without a closed-form solution of (3.2), but they would become more cumbersome to manipulate.

Using the asymptotics of (3.2) as $\mathcal{U}_0 \to 0$ shows that the structure near the wetting interface is given by

$$\mathcal{U}_0(\xi) \sim (-n\mathrm{Pe}\xi)^{1/n}, \qquad \text{as } \xi \to 0^-. \tag{3.4}$$

In Section 4, we will see that the Boltzmann similarity solution for the starting flow has a similar form at the wetting interface. Studying (3.3) for $\mathcal{U} \to 1$ shows that

$$\mathcal{U}_0(\xi) \sim 1 - \frac{1}{n}\mathrm{e}^{n\mathrm{Pe}\xi}, \qquad \text{as } \xi \to -\infty, \tag{3.5}$$

therefore the width of the front becomes narrower as n and the Peclet number increase.

4. The starting flow

4.1. Initial stage

The initial stage of the evolution describes the entry of moisture into the soil layer from the uniform source for very short times. Initially the solution will exhibit a large gradient in u over a small interval. We exploit this structure of the solution to describe the starting flow regime of the dynamics, from $t = 0$ until the eventual convergence to a traveling wave.

Let ϵ describe the spatial scale on which u varies from the boundary condition $u(0, t) = 1$ to $u = 0$ at the wetting interface position, $x = x_w(t)$. Substituting the scalings $\tilde{x} = x/\epsilon$ and $\tau = t/\epsilon^2$ in (2.12), we have

$$\frac{\partial u}{\partial \tau} + \epsilon \frac{\partial}{\partial \tilde{x}}\left(u^{n+1}\right) = \frac{1}{\mathrm{Pe}}\frac{\partial}{\partial \tilde{x}}\left(u^n \frac{\partial u}{\partial \tilde{x}}\right), \tag{4.1}$$

with initial and boundary conditions,

$$u(0, \tau) = 1, \qquad u(\tilde{x}, 0) = 0. \tag{4.2}$$

The parameter ϵ is called an artificial parameter since it was introduced by an arbitrary scaling and can just as easily be completely eliminated. Artificial parameter expansions can be shown to be non-uniformly convergent in time [25, Chapter 3], [33], [34, Chapter 3]. Hence, our solution will be good only for a limited time, but this situation can be improved somewhat by going to higher orders. This approach will be sufficient for our proposes to demonstrate transitions in the asymptotic behavior of the solution and to obtain improved estimates for quantities of interest. We will make use of analytical results by others in regard to the long-time behavior of the solution in various regimes.

As $\epsilon \to 0$, at leading order the convective term is absent and (4.1) reduces to a Dirichlet problem for the porous-medium equation,

$$\frac{\partial u_0}{\partial \tau} = \frac{1}{\mathrm{Pe}}\frac{\partial}{\partial \tilde{x}}\left(u_0^n \frac{\partial u_0}{\partial \tilde{x}}\right), \tag{4.3}$$

subject to (4.2). The solution of this leading-order problem is a Boltzmann similarity solution of the form, $u_0(\tilde{x}, \tau) = \mathcal{V}_0(\tilde{x}/\sqrt{\tau})$, where $\mathcal{V}_0(\eta)$ satisfies

$$\tfrac{1}{2}\eta \frac{\mathrm{d}\mathcal{V}_0}{\mathrm{d}\eta} + \frac{1}{\mathrm{Pe}} \frac{\mathrm{d}}{\mathrm{d}\eta}\left(\mathcal{V}_0^n \frac{\mathrm{d}\mathcal{V}_0}{\mathrm{d}\eta}\right) = 0, \qquad \mathcal{V}_0(0) = 1, \tag{4.4}$$

with $\eta = \tilde{x}/\sqrt{\tau}$. For the ubiquitous linear problem ($n = 0$), this solution is $\mathcal{V}_0(\eta) = \mathrm{erfc}(\frac{1}{2}\eta/\sqrt{\mathrm{Pe}})$. For the nonlinear porous-medium equation with $n > 0$, this solution has compact support with a well-defined interface position that moves with a finite speed [18, 19, 28].

Here the wetting interface is given by $x_w(t) = \eta_w\sqrt{t}$, where η_w is a constant. The appropriate form of the interface condition (2.15) is then

$$\tfrac{1}{2}\eta_w = -\frac{1}{\mathrm{Pe}}\mathcal{V}_0^{n-1}\frac{\mathrm{d}\mathcal{V}_0}{\mathrm{d}\eta}\bigg|_{\eta\to\eta_w^-} \qquad \mathcal{V}_0(\eta_w) = 0. \tag{4.5}$$

We can scale the Peclet number out of this problem by using $\eta \to \hat{\eta}/\sqrt{\mathrm{Pe}}$, so the solution of the leading-order problem (4.4, 4.5) only depends on n. There is no general closed-form solution of this problem for $n > 0$ [35], so in practice we solve (4.4, 4.5) numerically as a one-parameter shooting problem. In Figure 3b, we show numerical calculations for the interface position, η_w as a function of n; it is a monotone decreasing function that diverges to infinity as $n \to 0$. We can gain analytical insight into this behavior by considering the asymptotics for $n \to \infty$ as done in [22]. Similar to the approach used in [21] for $n \to 0$, consider the change of variables,

$$\mathcal{V}_0(\eta) = V^{1/n}(y), \qquad \eta = \frac{y}{\sqrt{n\mathrm{Pe}}}. \tag{4.6}$$

Then the moving-boundary problem for (4.4) becomes

$$VV'' + \frac{1}{n}\left(\tfrac{1}{2}yV' + V'^2\right) = 0, \qquad 0 \le y \le y_w, \tag{4.7}$$

subject to the boundary conditions,

$$V(0) = 1, \qquad V(y_w) = 0, \qquad V'(y_w) = -\tfrac{1}{2}y_w. \tag{4.8}$$

Expanding $V(y)$ and y_w in regular perturbation series, as $n \to \infty$, we obtain the solution of the moving boundary problem as

$$V(y) \sim \left(1 - \frac{y}{\sqrt{2}}\right) + \frac{y}{8n}(3\sqrt{2} - 2y) - \frac{\sqrt{2}y}{192n^2}(77 - 36\sqrt{2}y + 4y^2), \tag{4.9}$$

with the interface given by

$$y_w \sim \sqrt{2} + \frac{1}{\sqrt{8}\,n} - \frac{19\sqrt{2}}{96n^2}. \tag{4.10}$$

This result, in an equivalent form, was previously derived by King in [22]. Figure 3a shows the excellent agreement of (4.9) even for moderate values of n with the numerically calculated solution of (4.4). Figure 3b shows the comparison of (4.10) with the calculated wetting interface over a wide range of values for n.

More generally, we could extend the similarity variables suggested by this solution to include transient behavior with the timescale $s = \log(t)$. Then we can write $u(\tilde{x}, \tau) = \mathcal{V}(\eta, s)$, and (4.1) transforms to

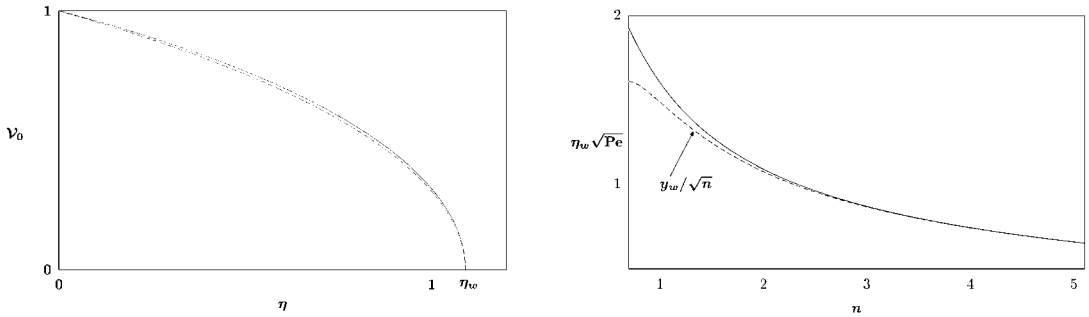

Figure 3. (left) The numerically calculated similarity solution $\mathcal{V}_0(\eta)$ of (4.4) for $n = 2$ (solid) compared with the three-term asymptotic solution (4.9) for $n \to \infty$ (dashed curve). (right) The numerically calculated wetting front coefficient η_w (solid) compared with the three-term asymptotic result (4.10) (dashed curve) as a function of n.

$$\frac{\partial \mathcal{V}}{\partial s} = \tfrac{1}{2}\eta\frac{\partial \mathcal{V}}{\partial \eta} + \frac{1}{\mathrm{Pe}}\frac{\partial}{\partial \eta}\left(\mathcal{V}^n\frac{\partial \mathcal{V}}{\partial \eta}\right) - \epsilon \mathrm{e}^{s/2}\frac{\partial}{\partial \eta}\left(\mathcal{V}^{n+1}\right). \tag{4.11}$$

We can seek the solution of this problem as a regular perturbation expansion, $\mathcal{V}(\eta, s) = \mathcal{V}_0(\eta) + \epsilon\mathcal{V}_1(\eta, s) + O(\epsilon^2)$. At $O(\epsilon)$, the problem for $\mathcal{V}_1$ is

$$\frac{\partial \mathcal{V}_1}{\partial s} = \mathcal{L}\mathcal{V}_1 - \mathrm{e}^{s/2}\frac{\partial}{\partial \eta}\left(\mathcal{V}_0^{n+1}\right), \tag{4.12}$$

where $\mathcal{L}f = \frac{1}{2}\eta\partial_\eta f + \partial_{\eta\eta}(\mathcal{V}_0^n f)/\mathrm{Pe}$. In the absence of the inhomogeneous forcing term, (4.12) is the equation for the linear stability analysis of the similarity solution $\mathcal{V}_0(\eta)$. The similarity solution $\mathcal{V}_0(\eta)$ is an asymptotic attractor for the porous-medium equation (4.3) [19, 36–38]. Hence $\mathcal{L}$ is a stable linear operator with only negative eigenvalues. Consequently, the dominant contribution to $\mathcal{V}_1$ is given by the convective forcing term and $\mathcal{V}_1$ exhibits unstable growth as $s \to \infty$, $\mathcal{V}_1 = O(\mathrm{e}^{s/2})$.

For $\tau \to \infty$, the solution of (4.3) converges to the similarity solution, possibly with a shifted time, $\tau \to \tau+\phi$ in the argument, *i.e.*, $u_0(\tilde{x}, \tau) \to \mathcal{V}_0(\tilde{x}/\sqrt{\tau+\phi})$ for different possible initial data [39]. This continuous, one-parameter family of solutions reflects the invariance of the PDE (4.3) with respect to time-shifts. We can write this family of solutions in terms of the similarity variables as

$$\mathcal{V}(\eta, s) = \mathcal{V}_0([1 + \phi\mathrm{e}^{-s}]^{-1/2}\eta). \tag{4.13}$$

For infinitesimal time shifts, $\phi \to 0$, these solutions can be expanded to provided linearized eigenmodes connected to the time-shift symmetry,

$$\mathcal{V}(\eta, s) \sim \mathcal{V}_0(\eta) + \phi\hat{\mathcal{V}}_T(\eta)\mathrm{e}^{\lambda_T s} \qquad \hat{\mathcal{V}}_T(\eta) = \tfrac{1}{2}\eta\mathcal{V}_0'(\eta) \qquad \lambda_T = -1. \tag{4.14}$$

We now make use of this one-parameter family of solutions to motivate a different form of perturbation expansion for the solution of (4.1), one which offers some benefits over the regular series in $\mathcal{V}$ described above.

When the specific initial data are neglected, the general similarity solution of (4.3) is

$$u_0(\tilde{x}, \tau) = \mathcal{V}_0\left(\frac{\tilde{x}}{\sqrt{\tau+\phi}}\right). \tag{4.15}$$

This can be regarded as the leading-order term in a multiple-scale expansion [25, Chapter 4] of the solution, where ϕ is a slowly varying phase function with $\phi = 0$ at $\tau = 0$ to satisfy

the initial conditions. The natural slow-space and slow-time variables for Equation (4.1) are in fact the original space and time scales, $x = \epsilon\tilde{x}$ and $t = \epsilon^2\tau$. However, when it is assumed that ϕ is a function of the slow variables alone, $\phi = \phi(x, t)$ turns out to be too restrictive; ϕ must be be slowly varying compared to τ, but as we will see in this problem, to balance the convective term ϕ can not be independent of τ. Recall that problem (4.1) is expressed in terms of an artificial small parameter. Consequently, the final form of the solution must be independent of this arbitrary parameter. In this context, we note that the combination of the slow variables, $x/\sqrt{t} = \eta$ is independent of ϵ. Proceeding formally, by substituting (4.15) into (4.1), we find that ϕ can be expressed in terms of the series

$$\phi(x, t, \tau) \sim \epsilon\tau^{3/2} \sum_{k=0}^{\infty} \epsilon^k \tau^{k/2} \phi_k(\eta). \tag{4.16}$$

Note that for $\epsilon \to 0$, the expansion of (4.15, 4.16) yields $u \sim \mathcal{V}_0(\eta) - \epsilon\phi_0(\eta)\mathrm{e}^{s/2}\hat{\mathcal{V}}_T(\eta)$, hence we can identify the $O(\epsilon)$ term with $\mathcal{V}_1(\eta, s)$ in the regular expansion used for (4.12). Hence, the problem for $\phi_0(\eta)$ is of the same form as solving (4.12) using variation of parameters. The boundary conditions for this problem would be that $\phi_0(0)$ is finite and $\eta_w\phi_0'(\eta_w) + 3\phi_0(\eta_w) = 0$, from expanding (2.15) to next order.

There are several benefits of using this form of expansion (4.15, 4.16). Having ϕ depend on space and time allows us to represent time-shifts in the evolution of the leading-order solution and deformations in its profile in a more compact form. It also gives the position of the wetting interface in a very convenient form (see Figure 4),

$$x_w(t) \sim \eta_w\sqrt{t + \phi_0(\eta_w)t^{3/2} + \phi_1(\eta_w)t^{5/2} + \ldots}. \tag{4.17}$$

Since (4.15) is an exact solution of the leading-order problem for all ϕ, not just $\phi \to 0$, see (4.14), it might be hoped that this form can reduce the magnitude of the higher-order corrections needed and yield a more accurate leading-order approximation. Finally, we briefly mention another possible form for the perturbation expansion of the solution motivated by multiple-scale analysis: the strained coordinate or Poincare-Lindstedt expansion [25, Chapter 4]. Here, the solution combines the form of a regular perturbation expansion,

$$u(\tilde{x}, \tau) = \mathcal{V}_0(\tilde{\eta}) + \epsilon\tilde{\mathcal{V}}_1(\tilde{\eta}, s) + O(\epsilon^2), \tag{4.18}$$

with a slowly varying phase correction,

$$\tilde{\eta} = \tilde{x}/\sqrt{\tau + \tilde{\phi}(t, \tau)}, \qquad \phi(t, \tau) \sim \epsilon\tau^{3/2} \sum_{k=0}^{\infty} \tilde{\phi}_k \epsilon^k \tau^{k/2}, \tag{4.19}$$

where the constants $\tilde{\phi}_k$ are obtained by applying appropriate solvability conditions to the functions $\tilde{\mathcal{V}}_{k+1}$. While the forms of these expansions are well-motivated by the form of the general solution (4.15), further analysis remains to be done to determine if they remain valid over longer regimes than a regular perturbation expansion.

4.2. Convergence to the wetting-front traveling wave

The next regime of behavior for the solution occurs at long times after the Boltzmann solution has de-stabilized but before the wetting interface has reached the edge of the domain at $x = 1$. In [16], it was shown that the solution of the initial-boundary-value problem for (2.12), (2.14)

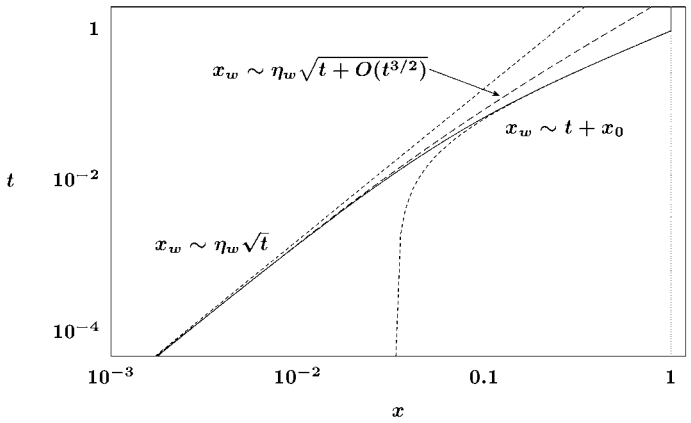

Figure 4. Motion of the wetting interface (solid curve) during the starting flow regime along short and long time asymptotic behaviors (dashed curves).

and boundary condition $u(0,t) = 1$ on the semi-infinite domain, $x \geq 0$, converges asymptotically to a traveling-wave solution of the form in Section 3 as $t \to \infty$. Due to the degenerate form of (2.12), before the wetting interface reaches $x = 1$, the boundary condition at $x = 1$, (2.13), does not influence the flow and hence until that time the domain is effectively semi-infinite. Therefore, we can apply the results of Vanaja and Sachdev to estimate the convergence to the traveling wave in finite time, $0 \leq t < t_w$, where $x_w(t_w) = 1$. Here we will briefly show that the rate of convergence improves as the Peclet number increases.

To examine the convergence $u(x,t) \to \mathcal{U}_0(x - t + \theta)$, where θ is a phase constant to account for translation invariance, we write (2.12) in a moving reference frame for $u = \mathcal{U}(\xi, t)$,

$$\frac{\partial \mathcal{U}}{\partial t} - \frac{\partial \mathcal{U}}{\partial \xi} + \frac{\partial}{\partial \xi}\left(\mathcal{U}^{n+1}\right) = \frac{1}{\mathrm{Pe}}\frac{\partial}{\partial \xi}\left(\mathcal{U}^n \frac{\partial \mathcal{U}}{\partial \xi}\right). \tag{4.20}$$

As described in [20, Chapter 7], classic linear stability analysis of the traveling wave assumes a solution of the form $\mathcal{U} \sim \mathcal{U}_0(\xi) + \epsilon \mathcal{U}_1(\xi, t)$ to then yield a linearized eigenvalue problem for $\mathcal{U}_1$. The translation symmetry $x \to x + \theta$ of the traveling wave yields a neutrally stable mode, given by linearizing $\mathcal{U}(\xi + \theta)$ for $\theta \to 0$,

$$\mathcal{U}(\xi, t) \sim \mathcal{U}_0(\xi) + \theta \hat{\mathcal{U}}_T(\xi) \mathrm{e}^{\lambda_T t}, \qquad \hat{\mathcal{U}}_T = \mathcal{U}_0'(\xi), \qquad \lambda_T = 0. \tag{4.21}$$

Here, instead, we consider perturbations to monotone traveling waves in terms of a phase function,

$$u = \mathcal{U}_0(\xi + \theta(\xi, t)\,). \tag{4.22}$$

Again, it can be hoped that this form can extend the range of validity of the linearized model from infinitesimal perturbations. In particular, we again note that this form gets translation invariance correct for all θ, not just for infinitesimal translations, $\theta \to 0$.

In fact, comparison of (4.22) and the classical linear stability *ansatz* shows that the linearized eigenvalue problems for both cases are equivalent – they yield the same eigenvalues and the eigenfunctions differ by a multiplicative weight function derived from $\mathcal{U}_0(\xi)$. Let the phase be $\theta(\xi, t) \sim -x_0 + \epsilon \hat{\theta}(\xi) \mathrm{e}^{\lambda t}$ and exclude consideration of the translation mode. Then, the exponential growth rate of perturbations is given by $\lambda = \mathrm{Pe}\,\tilde{\lambda}$ and $\hat{\theta}(\xi)$ satisfies the eigenvalue problem

$$(1 - \mathrm{e}^{n\mathrm{Pe}\xi})\hat{\theta}'' + (n\mathrm{Pe} - (n+1)\mathrm{Pe}\,\mathrm{e}^{n\mathrm{Pe}\xi})\hat{\theta}' - \mathrm{Pe}^2\tilde{\lambda}\hat{\theta} = 0, \qquad -\infty < \xi \leq 0. \tag{4.23}$$

To show that $\tilde{\lambda}$ is independent of Pe, we use the change of variables, $\hat{\theta}(\xi) = \hat{\Theta}(z)$ where $z = \mathrm{e}^{n\mathrm{Pe}\xi}$, to obtain the singular eigenvalue problem for $\hat{\Theta}(z)$,

$$n^2z^2(1-z)\hat{\Theta}'' + (2n(1-z) - z)nz\hat{\Theta}' - \tilde{\lambda}\hat{\Theta} = 0, \qquad 0 \leq z \leq 1. \tag{4.24}$$

The solutions of this problem can be expressed in terms of hypergeometric functions, and from the results of [16], the eigenvalues are stable. Hence it is clear that the decay rate of the dominant mode is $\mathrm{Pe}\,\tilde{\lambda}_1 = O(\mathrm{Pe})$.

5. The stopping behavior

From the results of the previous section, if Pe is sufficiently large, then by the time that the wetting interface reaches the far edge of the soil layer at $x = 1$, we may assume that the solution has converged to the traveling-wave solution. In this section we examine the short-time behavior after the traveling wave first feels the influence of the no-flux boundary at $x = 1$. Due to this boundary, the wave will stop propagating and change in profile; this was described as a 'stopping' behavior in [23, 24].

Assume that the wetting interface reaches $x = 1$ at the known time $t = t_w$; then for short times before t_w, the solution is

$$u(x,t) = \mathcal{U}_0(x - t + \theta_w), \qquad \theta_w = t_w - 1, \tag{5.1}$$

where the phase θ_w has been chosen so that $u(1, t_w) = 0$. To study the subsequent behavior for short times in a neighborhood of the boundary, let ϵ be an artificial small parameter corresponding to the timescale we wish to consider, then rescale space and time according to

$$x = 1 + \epsilon\tilde{x}, \qquad t = t_w + \epsilon\tau. \tag{5.2}$$

In absence of the boundary condition at $x = 1$, the outer solution determines the scaling of u to be

$$u(1,t) = \mathcal{U}_0(1 - t + \theta_w) = \mathcal{U}_0(\epsilon\tilde{x} - \epsilon\tau) = O(\epsilon^{1/n}), \tag{5.3}$$

as $\epsilon \to 0$ for $t > t_w$. Therefore, in the neighborhood of $x = 1$, we rescale u by

$$u = \epsilon^{1/n}\tilde{u}(\tilde{x}, \tau). \tag{5.4}$$

Consequently, the governing equation (2.12) becomes

$$\frac{\partial\tilde{u}}{\partial\tau} + \epsilon\frac{\partial}{\partial\tilde{x}}\left(\tilde{u}^{n+1}\right) = \frac{1}{\mathrm{Pe}}\frac{\partial}{\partial\tilde{x}}\left(\tilde{u}^n\frac{\partial\tilde{u}}{\partial\tilde{x}}\right), \tag{5.5}$$

on $-\infty < \tilde{x} \leq 0$, with the no-flux boundary condition

$$\left.\frac{1}{\mathrm{Pe}}\frac{\partial\tilde{u}}{\partial\tilde{x}}\right|_{\tilde{x}=0} = \epsilon\tilde{u}(0,\tau). \tag{5.6}$$

While (5.5, 5.6) does not take the classic form of a singularly perturbed boundary-value problem [25, Chapter 2], the solution does include a localized boundary-layer correction marking the onset of the influence of the no-flux boundary at $x = 1$, as described in [23, 24]. This boundary layer accompanies the change in the character of the solution from having compact support due to degenerate diffusion to being uniformly parabolic when $u > 0$ everywhere. In the former case, the boundary condition at $x = 1$ has no effect on the flow until it comes in contact with the wetting interface. In the latter case, the details of the boundary condition are necessary to specify a unique solution of the convection-diffusion equation (5.5).

Following the approach used to study the starting flow in Section 4, we will describe the stopping behavior in terms of the underlying solution of the outer problem with a phase function to capture the influence of the perturbations due to the boundary for $\tau > 0$,

$$\tilde{u}(\tilde{x}, \tau) = \epsilon^{-1/n} \mathcal{U}_0(\epsilon\tilde{x} - \epsilon\tau + \tilde{\theta}(\tilde{x}, \tau)), \tag{5.7}$$

where for $\tau \leq 0$, the phase is $\tilde{\theta}(\tilde{x}, \tau) \equiv 0$ to recover (5.1). This will serve as our *ansatz* for the inner solution of (5.5).

As in the case of the phase correction (4.16) to the Boltzmann similarity solution for the starting flow, we can write $\tilde{\theta}$ as a time series of the form,

$$\tilde{\theta}(\tilde{x}, \tau) \sim \epsilon\tau \sum_{k=0}^{\infty} \epsilon^k \tau^k \tilde{\theta}_k(\zeta), \qquad \zeta = \tilde{x}/\tau, \tag{5.8}$$

where the new similarity variable ζ is independent of the artificial small parameter ϵ; see (5.2). Consequently, all of the coefficient functions $\tilde{\theta}_k(\zeta)$ are $O(1)$ as $\epsilon \to 0$.

Substitution of (5.7, 5.8) in (5.5, 5.6) yields the leading order problem for $\tilde{\theta}_0(\zeta)$ on $-\infty < \zeta \leq 0$,

$$\mathcal{N}(\tilde{\theta}_0) \equiv n(1 - \zeta - \tilde{\theta}_0)\tilde{\theta}_0'' + (\zeta - 2 - \tilde{\theta}_0')\tilde{\theta}_0' - \tilde{\theta}_0 = 0, \tag{5.9}$$

with boundary conditions for matching to the outer solution and satisfying the no-flux condition,

$$\tilde{\theta}_0(\zeta \to -\infty) \to 0, \qquad \tilde{\theta}_0'(0) = -1. \tag{5.10}$$

Equation (5.9) has a special closed-form solution, and using symmetry methods, we can reduced it to a first-order Abel equation, yet neither of these observations are helpful for solving the boundary-value problem subject to (5.10). However, it is helpful to study the local behavior of solutions of (5.9), which yields that as $\zeta \to 0$, $\tilde{\theta}_0(y) \sim \tilde{\theta}_0(0) - \zeta - \zeta^2/(2n)$, and as $\zeta \to -\infty$, $\tilde{\theta}_0(y) \sim C\zeta^{-1}\exp(\zeta/n)$. Consequently, we can find exponentially localized solutions of (5.9, 5.10) from a one-parameter numerical shooting method in terms of the value $\tilde{\theta}_0(0)$.

Over a wide range in values of n, to a good approximation, the numerical results show that $\tilde{\theta}_0(0)$ is linear in n, that is $\tilde{\theta}_0(0) \approx \omega n$, where roughly $\omega \approx -3/4$. This rather distinctive behavior can be extracted semi-analytically from (5.9) in terms of the rescaled variables, $\tilde{\theta}_0(\zeta) = n\Theta(z)$ where $\zeta = nz$. Then the problem becomes

$$(\Theta + z)\Theta'' - z\Theta' + \Theta - \frac{1}{n}\left[\Theta'' - (\Theta' + 2)\Theta'\right] = 0, \tag{5.11}$$

$$\Theta(z \to -\infty) \to 0, \qquad \Theta'(0) = -1. \tag{5.12}$$

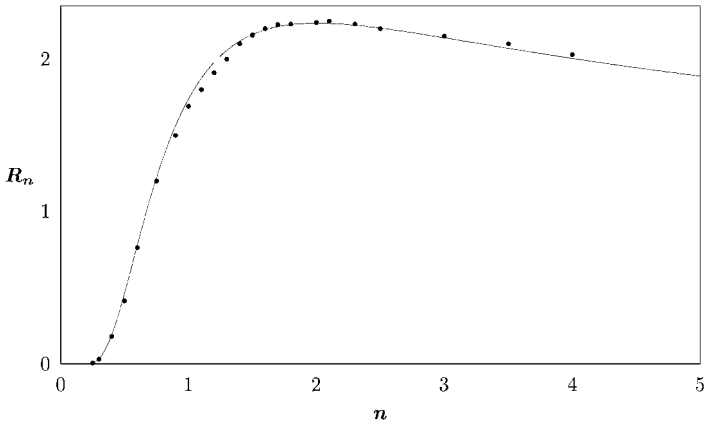

Figure 5. Comparison of the asymptotic solution for the moisture accumulation rate constant R_n (5.14) (curve) with results from direct numerical solutions of Richards' equation (2.12) at various n's (dots).

We expand $\Theta(z) = \Theta_0(z) + \Theta_1(z)/n + O(n^{-2})$ in the limit $n \to \infty$. The leading-order problem for $\Theta_0(z)$ must still be solved numerically, but it provides us with an estimate that can be applied for a wide range of values of n, $\omega \sim \Theta_0(0) \approx -0{\cdot}7717894686$.

Use of these results for $\tilde{\theta}_0(0)$ in (5.7, 3.4) yields an estimate for initial rate of accumulation of moisture at the no-flux boundary at $t = t_w$,

$$u(1, t \to t_w) \sim R_n(t - t_w)^{1/n}, \tag{5.13}$$

where

$$R_n = (n[1 - \tilde{\theta}_0(0)])^{1/n} \approx (n + 0{\cdot}772n^2)^{1/n}. \tag{5.14}$$

The dependence of R_n on n is non-trivial; it has a maximum near $n = 2$, a super-exponential decay $R_n \sim \mathrm{e}^{0{\cdot}772}n^{1/n}$ as $n \to 0$, and a slow decay for large n. This behavior was verified by comparison with results from numerical simulations of Richards' equations at various values of n, see Figure 5.

The leading-order problem (5.9) for $\tilde{\theta}_0(\zeta)$ was first considered in [24]. It was noted that truncating the expansion of $\tilde{\theta}$ to $\tilde{\theta}_0$ corresponds to neglecting the influence of the convective term in the PDE and replacing the no-flux Robin boundary condition by a Neumann condition. That is, the leading-order estimate is given by solving the horizontal infiltration problem,

$$\frac{\partial u}{\partial t} = \frac{\partial}{\partial x}\left(u^n \frac{\partial u}{\partial x}\right), \qquad \left.\frac{\partial u}{\partial x}\right|_{x=1} = 0. \tag{5.15}$$

This is in agreement with arguments described by Parlange [40] reducing Richards' equation to the porous medium equation for horizontal infiltration, by neglecting the convective effect of gravity when a wetting front first arrives at a soil stratification boundary [40–42]. However, this observation also makes it clear that there is a need to go to higher orders in the expansion of $\tilde{\theta}$ to properly describe: the influence of the no-flux boundary condition, the convective contribution due to gravity, and the longer-time rate of accumulation of moisture at $x = 1$.

In calculating the higher order corrections to (5.8), we get a series of linear problems for $\tilde{\theta}_k(\zeta)$ in terms of the operator

$$\mathcal{L}_k\tilde{\theta}_k \equiv \left[\frac{\delta\mathcal{N}}{\delta\theta} - k\right]\tilde{\theta}_k = n(1 - \zeta - \tilde{\theta}_0)\tilde{\theta}_k'' + (\zeta - 2 - 2\tilde{\theta}_0')\tilde{\theta}_k' - (n\tilde{\theta}_0'' + 1 + k)\tilde{\theta}_k. \tag{5.16}$$

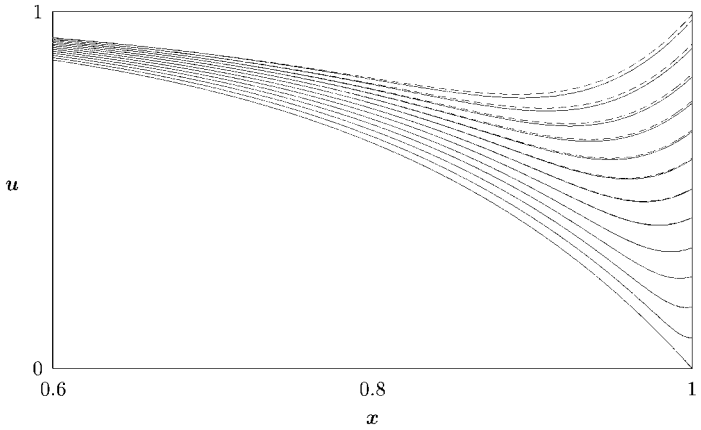

Figure 6. Details of the stopping behavior in a neighborhood of the no-flux boundary at $x = 1$: numerical solutions (solid curves) and the three-term uniform asymptotic solution (5.22) (dashed) given at corresponding times.

Note that this is *not* the linearized operator for (5.9). The difference is due to the form (5.7) in which we are seeking our perturbation solution, where $\tilde{\theta}$ is a modification to the phase of the traveling wave, rather than a linear perturbation of the outer solution. The $O(\epsilon)$ problem is

$$\mathcal{L}_1\tilde{\theta}_1 = -\tfrac{1}{2}n\mathrm{Pe}(1-\zeta-\tilde{\theta}_0)\left[(2n+1)\tilde{\theta}_0'^2 + (2n+\zeta)\tilde{\theta}_0' - \tilde{\theta}_0\right], \tag{5.17}$$

$$\tilde{\theta}_1(\zeta \to -\infty) \to 0, \qquad \tilde{\theta}_1'(0) = -n\mathrm{Pe}(1-\tilde{\theta}_0(0)). \tag{5.18}$$

The solution of this problem scales with the Peclet number, $\tilde{\theta}_1(\zeta) = \mathrm{Pe}\bar{\theta}_1(\zeta)$, so the problem for $\bar{\theta}_1(\zeta)$ is independent of Pe. In fact, using the scaling

$$\tilde{\theta}_k(\zeta) = \mathrm{Pe}^{\,k}\bar{\theta}_k(\zeta), \tag{5.19}$$

in the perturbation expansion (5.8) of $\tilde{\theta}(\xi,\tau)$ makes all of the linear problems for the higher order corrections independent of Pe.

We note that (5.7) is convenient representation for the *inner solution* of (5.5) in the neighborhood of $x = 1$ that reduces the matching conditions to making $\tilde{\theta}$ vanish as $\zeta \to -\infty$. However, to construct a solution that is uniformly valid in space describing the stopping behavior, we must make use of ideas from matched asymptotic expansions [25, Chapter 2], [34, Chapter 2]. In short, a uniform solution can be constructed from the sum of the inner and outer solutions minus the overlap of the two in terms of a common set of variables. The outer solution, (5.1), is valid for $0 \le x < 1$, and in terms of the time-variable τ, it is $u \sim \mathcal{U}_0(x-\epsilon\tau-1)$. Similarly, we write the inner solution, (5.7), in terms of the outer spatial variable x as $u \sim \mathcal{U}_0(x-1-\epsilon\tau+\tilde{\theta})$, where $\tilde{\theta}$ depends explicitly on ϵ as shown in (5.8), but ζ is scale-independent of ϵ. Then both of these solutions are expanded in powers of ϵ, and the common terms are identified to yield the uniformly valid solution. This procedure is straightforward for general n, though the algebraic expressions are somewhat unwieldy, so we briefly present only the special case for $n = 1$ as an example. For $n = 1$, the expansion of the outer solution is

$$u_{\mathrm{out}} \sim 1 - \mathrm{e}^{\mathrm{Pe}(x-1)}\mathrm{e}^{-\mathrm{Pe}\epsilon\tau} \sim 1 - \mathrm{e}^{\mathrm{Pe}(x-1)}\left(1 - \epsilon\tau\mathrm{Pe} + \tfrac{1}{2}\epsilon^2\tau^2\mathrm{Pe}^2\right), \tag{5.20}$$

while the expansion of the inner solution is

$$u_{\text{in}} \sim 1 - \mathrm{e}^{\mathrm{Pe}(x-1)} \left(1 - \epsilon\tau \mathrm{Pe}[1 - \bar{\theta}_0(\zeta)] + \frac{1}{2}\epsilon^2\tau^2 \mathrm{Pe}^{\,2} \left[1 - 2\bar{\theta}_0(\zeta) + \bar{\theta}_0^2(\zeta) + 2\bar{\theta}_1(\zeta) \right] \right). \tag{5.21}$$

Consequently, the $O(\epsilon^2)$ accurate uniformly valid solution for $\tau \to 0^+$ is

$$u \sim 1 - \mathrm{e}^{\mathrm{Pe}(x-1)} \left(\mathrm{e}^{\epsilon\tau \mathrm{Pe}\tau} + \epsilon\tau \mathrm{Pe}\bar{\theta}_0(\zeta) + \tfrac{1}{2}\epsilon^2\tau^2 \mathrm{Pe}^2[\bar{\theta}_0^2(\zeta) + 2(\bar{\theta}_1(\zeta) - \bar{\theta}_0(\zeta))] \right), \tag{5.22}$$

where $\zeta = (x-1)/\tau$. The excellent agreement between the three-term solution (5.22) and the results from the numerical solution of (2.12) are shown in Figure 6. The perturbation solution is accurate for even moderately large values of u in the boundary layer; the accuracy can be improved by retaining more terms in the expansion of $\tilde{\theta}$ (5.8). Moreover, using these results, we can extend the validity of the estimate of the moisture accumulation at the $x = 1$ boundary (5.13) in the general form,

$$u(1, t \sim t_w) \sim R_n (t - t_w)^{1/n} \left(1 + \sum_{k=1} \tilde{c}_k (t - t_w)^k \right), \tag{5.23}$$

where the $\tilde{c}_k$ coefficients are given by algebraic combinations of $\bar{\theta}_k(0)$ and powers of Pe.

6. Reverse flow with saturation

From the results of previous section, we can calculate the solution for short to moderate times after the gravity current has impinged on the impervious boundary. As shown in Figure 6, the solution becomes non-monotone since the water accumulates rapidly in the neighborhood of $x = 1$. For longer times, the behavior at this boundary is the dominant mechanism controlling the flow, as water begins to back-propagate through the soil layer. In this section and the following one, we consider two forms of reverse flow (that, to the author's knowledge, have not previously appeared in the literature) that can occur following the stopping behavior regime.

We begin with the simpler case, when saturation occurs and drives the reverse flow. As described in Section 2, if the soil layer has a saturation level satisfying $u_s < \mathrm{e}^{\mathrm{Pe}}$, then Richards' equation (2.12) for unsaturated flow must be treated on a reduced domain, with an interface condition to the growing region of the layer where the soil is saturated. At a large, but finite time $t = t_s$, estimated by (5.23), the concentration of water will reach the saturation level, $u = u_s$, at $x = 1$. Starting from $x_s = 1$, the saturated region will spread upward through the layer, with a no flux boundary condition at the interface with the unsaturated flow (2.17).

Following time t_s there is a brief transient regime and then the solution rapidly converges to a constant-velocity saturation wave that we will focus on here. The later stages of the transient regime (the convergence to the traveling wave) can be treated similarly to the approach given in Section 4; the earlier stages of the behavior will be studied in more detail in Section 7. Here we will assume that the reverse flow has converged to a traveling wave, $u \to \mathcal{U}_s(x - c_s t + \theta)$, with $c_s < 0$ (see Figures 2 and 7).

The saturation wave satisfies equation (3.1) subject to the boundary conditions

$$u(0, t) = 1, \qquad u(x_s(t), t) = u_s > 1, \tag{6.1}$$

and the no flux condition (2.17) at $x_s(t)$. Integration of (3.1) and application of the boundary conditions yields the speed of the reverse flow,

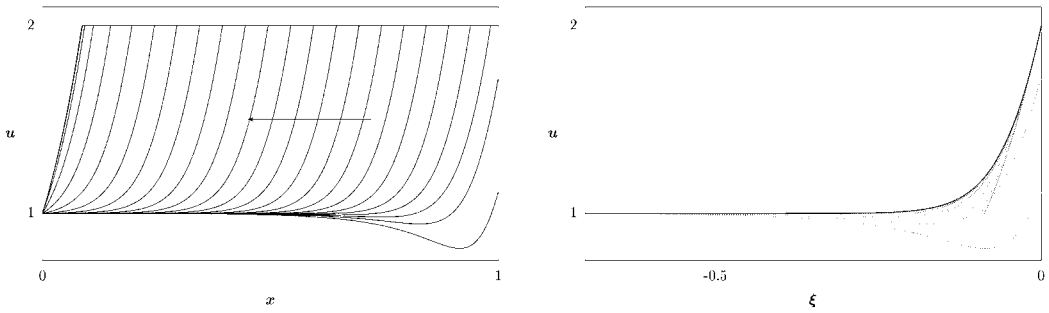

Figure 7. (left) Numerical calculation of the saturated reverse flow, with $u_s = 2$, showing propagating of a constant velocity wave. (right) Convergence of the same data (dotted curves) to a saturation wave given by the solution of (6.3) (solid curve), when viewed in the moving reference frame with $\xi = x - c_s t$. (The final few data curves show divergence from the intermediate asymptotic saturation wave and convergence to the long-time steady state solution.)

$$c_s = -\frac{1}{u_s - 1} < 0, \tag{6.2}$$

and the first order ordinary differential equation for the saturation front on $-\infty < \xi \leq 0$,

$$\frac{\mathrm{d}\mathcal{U}_s}{\mathrm{d}\xi} = \mathrm{Pe}\left[\mathcal{U}_s - \frac{1}{\mathcal{U}_s^n}\left(\frac{u_s - \mathcal{U}_s}{u_s - 1}\right)\right], \qquad \mathcal{U}_s(0) = u_s. \tag{6.3}$$

Note that $\mathcal{U}_s(\xi)$ is defined with the saturation interface at $\xi = 0$, with a uniformly saturated flow $u \equiv u_s$ for all $\xi > 0$. Neglecting the short transient leading to convergence to $\mathcal{U}_s$, we can write the solution as (see Figure 7)

$$u(x,t) \sim \mathcal{U}_s(x - x_s(t)), \qquad x_s(t) \sim 1 + c_s(t - t_s). \tag{6.4}$$

The saturation wave is the penultimate intermediate-asymptotic stage in the dynamics of this problem before the convergence to the steady state. As this wave propagates toward $x = 0$, eventually it will feel a 'stopping' influence (as in Section 5) due to the Dirichlet boundary condition at $x = 0$. However, if $n \gg 1$, we can see that this is a weak influence. Linearizing the solution for $\mathcal{U}_s \to 1$ yields

$$\mathcal{U}_s(\xi \to -\infty) \sim 1 + \epsilon \exp\left[\mathrm{Pe}\left(n + \frac{u_s}{u_s - 1}\right)\xi\right]. \tag{6.5}$$

Thus, if $n > 1$ the saturation front profile approaches $u \to 1$ more rapidly as x decreases than the steady-state solution, $\bar{u}(x) = \mathrm{e}^{\mathrm{Pe}x}$. Hence the saturation wave moves toward $x = 0$ with relatively little 'stopping' influence until it approaches the width of the unsaturated steady state solution, $\bar{x}_s = \log(u_s)/\mathrm{Pe}$; see Figures 7 and 8.

7. Reverse flow without saturation

We conclude by briefly examining the case in which the saturation constraint does not come into play and as $t \to \infty$ the solution approaches the unsaturated steady state $\bar{u}(x) = \mathrm{e}^{\mathrm{Pe}x}$ in the entire layer. Here, we will use the assumption that $u \gg 1$ as $x \to 1$ to construct a quasi-steady solution when $n \gg 1$.

Let $u(x,t) = \tilde{u}(x,t)/\epsilon$, where ϵ is a small parameter, $\epsilon = O(\mathrm{e}^{-\mathrm{Pe}})$, then (2.12) becomes

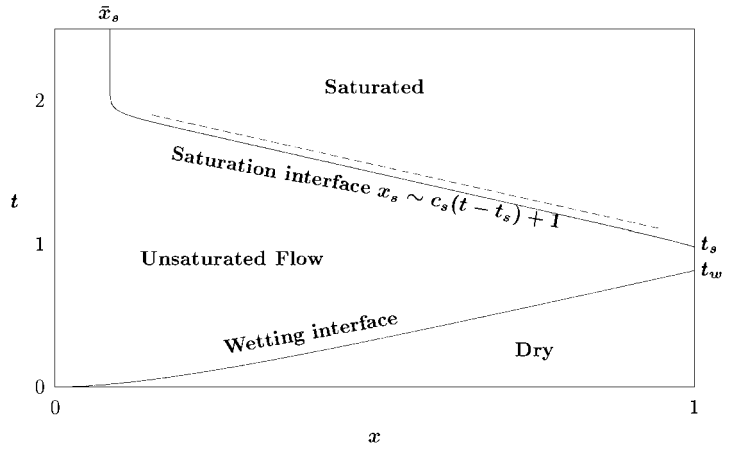

Figure 8. The space-time diagram showing regimes of no-flow (the dry state), unsaturated flow, and saturated flow and the interfaces separating those regions.

$$\epsilon^n \frac{\partial \tilde{u}}{\partial t} + \frac{\partial}{\partial x}\left(\tilde{u}^{n+1}\right) = \frac{1}{\mathrm{Pe}} \frac{\partial}{\partial x}\left(\tilde{u}^n \frac{\partial \tilde{u}}{\partial x}\right), \tag{7.1}$$

with the no-flux boundary condition,

$$\frac{1}{\mathrm{Pe}} \frac{\partial \tilde{u}}{\partial x}\bigg|_{x=1} = \tilde{u}(1, t). \tag{7.2}$$

The leading-order solution of this problem is $u_0(x, t) = C(t)\mathrm{e}^{\mathrm{Pe}x}$, where $C(t)$ is a as-yet undetermined function of time. It is more convenient to represent this coefficient function as $C(t) = \exp(-\mathrm{Pe}x_1(t))$, where $x_1(t)$ represents a moving boundary where the assumption that $u \gg 1$ breaks down. We can then approximate the structure of the solution by $u \approx 1$ to the left of $x_1(t)$, and overall

$$u_0(x, t) = \begin{cases} \exp(\mathrm{Pe}[x - x_1(t)]), & x_1(t) < x \leq 1, \\ 1 \qquad\qquad\qquad\quad , & 0 \leq x < x_1(t), \end{cases} \tag{7.3}$$

see Figure 9. Solution (7.3) may be regarding as a leading-order outer solution, valid everywhere away from a small neighborhood of $x_1(t)$. For $x \ll x_1$ the solution is essentially determined by the boundary condition $u(0, t) = 1$, for $x \gg x_1$ by (7.2), and continuous across x_1. As will be shown, details of the solution near x_1 are not needed to obtain the leading-order behavior. We note that in $x_1 < x \leq 1$, the solution is a quasi-steady propagating wave, it is given in terms of the equilibrium solution by

$$u(x, t) \sim \bar{u}(x - x_1(t)), \tag{7.4}$$

with the accumulation of moisture at the impervious boundary given by $u(1, t) \sim \bar{u}(1 - x_1(t))$.

The rate at which moisture accumulates at the boundary and at which the reverse flow propagates back toward the surface at $x = 0$ is controlled by the flux of moisture into the layer. The total mass of water in the layer is given by

$$m = \int_0^1 u(x, t)\, \mathrm{d}x, \tag{7.5}$$

From the PDE (7.3), and *ansatz* (7.3) while $x_1(t) > 0$, we have

$$\frac{\mathrm{d}m}{\mathrm{d}t} = \left(\frac{1}{\mathrm{Pe}}u^n u_x - u^{n+1}\right)\Big|_{x=0} \approx 1. \tag{7.6}$$

Similarly, direct substitution of (7.3) into (7.5) yields

$$\frac{\mathrm{d}m}{\mathrm{d}t} = \left(1 - \mathrm{e}^{\mathrm{Pe}(1-x_1)}\right)\frac{\mathrm{d}x_1}{\mathrm{d}t}. \tag{7.7}$$

Consequently, we can write a first-order differential equation for the evolution of $x_1(t)$, (see Figure 10)

$$\frac{\mathrm{d}x_1}{\mathrm{d}t} = -\frac{1}{\mathrm{e}^{\mathrm{Pe}(1-x_1)} - 1}. \tag{7.8}$$

It is notable that this solution is independent of n in contrast to the nature of the stopping behavior being strongly dependent on n and independent of Pe to leading order. For short times after the onset of this reverse flow regime, when $x_1(t_1) = 1$, the wave propagates as if it were purely diffusive,

$$x_1(t) \sim 1 - \sqrt{\frac{2(t-t_1)}{\mathrm{Pe}}}, \qquad \text{as } t \to t_1. \tag{7.9}$$

This makes for an interesting contrast with the constant speed propagation of the reverse-flow saturation front found in the previous section.

The final stage of the evolution occurs when $x_1(t) \to 0$ and the influence of the structure of the solution near the $x = 0$ boundary becomes significant. However, by this point in time, the difference between (7.3) and the equilibrium solution $\bar{u}(x)$ is relatively small, so linearized stability may be sufficient to describe the leading order dynamics. Using separation of variables, we can describe the evolution of infinitesimal perturbations to steady state by

$$u(x,t) = \mathrm{e}^{\mathrm{Pe}x} + \epsilon\hat{w}(x)\mathrm{e}^{-(n-1)\mathrm{Pe}x/2}\mathrm{e}^{-\lambda^2 t}, \qquad \text{as } t \to \infty, \tag{7.10}$$

where the eigenfunction $\hat{w}(x)$ on $0 \le x \le 1$ satisfies the boundary-value problem,

$$\hat{w}'' - \left(\frac{\mathrm{Pe}^{\,2}(n+1)^2}{4} - \lambda^2 \mathrm{Pe}\,\mathrm{e}^{-n\mathrm{Pe}x}\right)\hat{w} = 0, \tag{7.11}$$

$$\hat{w}(0) = 0, \qquad (n+1)\hat{w}(1) = \frac{2}{\mathrm{Pe}}\hat{w}'(1). \tag{7.12}$$

This is a self-adjoint Sturm-Liouville problem, so no unstable perturbation modes can occur. The solution of this problem is given in terms of Bessel functions, and (after using the boundary condition at $x = 0$) takes the form

$$\hat{w}(x) = \mathrm{Y}_\nu\left(\frac{2\lambda}{n\sqrt{\mathrm{Pe}}}\right)\mathrm{J}_\nu\left(\frac{2\lambda}{n\sqrt{\mathrm{Pe}}}\mathrm{e}^{-n\mathrm{Pe}x/2}\right) - \mathrm{J}_\nu\left(\frac{2\lambda}{n\sqrt{\mathrm{Pe}}}\right)\mathrm{Y}_\nu\left(\frac{2\lambda}{n\sqrt{\mathrm{Pe}}}\mathrm{e}^{-n\mathrm{Pe}x/2}\right). \tag{7.13}$$

Application of the other boundary condition, $\mathrm{Pe}(n+1)\hat{w}(1) = 2\hat{w}'(1)$, yields an equation to determine the eigenvalues λ, which all correspond to finite decay rates.

We note that with minor modifications this linear stability analysis for $t \to \infty$ could be applied to describe the final stages of the evolution of the reverse flow with saturation in Section 6, on the interval $0 \le x \le \bar{x}_s = \log(u_s)/\mathrm{Pe}$.

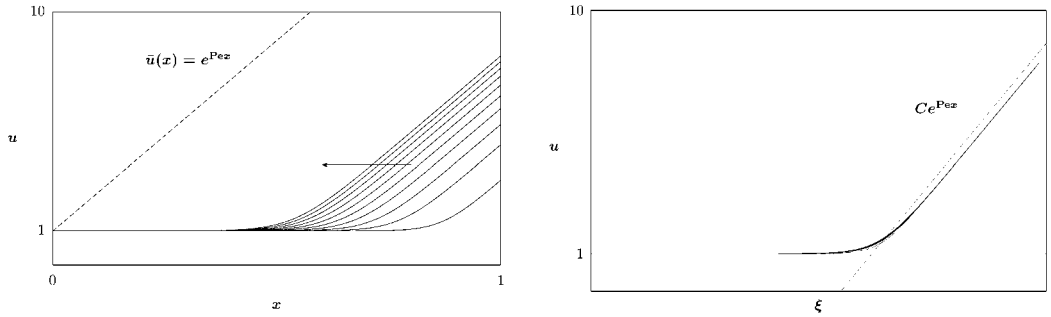

Figure 9. (left) Numerical calculation of the unsaturated reverse flow, showing the wave slowly approaching the steady state, (right) Collapse of the same data onto a single quasi-steady wave profile (7.3), when viewed in the moving reference frame $\xi = x - x_1(t)$.

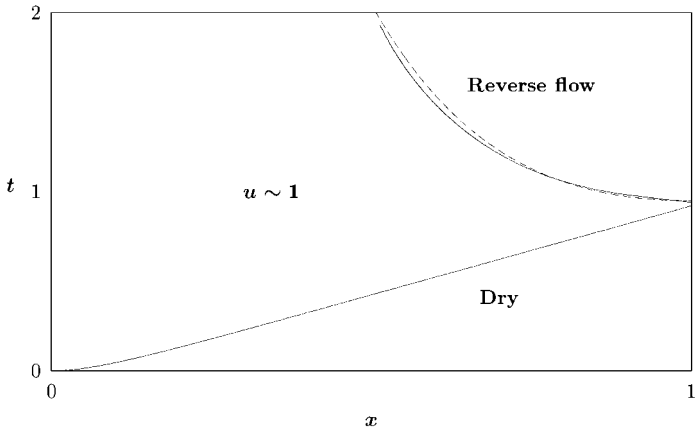

Figure 10. The space-time diagram for regimes in the dynamics without saturation. The wetting interface and the contour for $u \approx 1{\cdot}1$ are shown with solid curves. The $x_1(t)$ interface from (7.8) is shown as a dashed curve for comparison.

8. Conclusion

Thus, we have concluded the analysis of this vertical infiltration problem, bringing the solution from its behavior for $t \to 0$ through to the end, $t \to \infty$. Using perturbation methods, we constructed approximate solutions for all of the stages in the dynamics of this problem. While complete solution of this problem, taken as a whole, necessitates numerical simulation, using asymptotics to isolate the dominant influences governing each stage of evolution can yield much more insight regarding the structure of the solution. Reducing the full problem to obtaining an intermediate asymptotic solution for each stage makes careful mathematical analysis tractable. The examination of the linear stability and weakly-nonlinear dynamics of the asymptotic states in the full problem shows how dynamic transitions between stages develop and allows us to construct relations connecting the different stages of the dynamics. The problem for (1.1) studied here serves as a simple example of how this perturbation-method approach can be applied to quantitatively predict the dynamics in more general problems.

Acknowledgments

I would like to extend my very special thanks to Professor J.-Y. Parlange for suggesting this problem and for sharing his vast experience on problems in porous media. I also thank Andy Bernoff and Tim Green for very helpful discussions. This research was supported by a fellowship from the Alfred P. Sloan foundation.

References

1. J. Bear, *Dynamics of Fluids in Porous Media*. New York: Dover publications (1972) 764 pp.
2. P. Broadbridge, Moving boundary problems with nonlinear diffusion. In: R. S. Anderssen, J. M. Hill and A. K. Pani (eds.), *Mini-Conference on Free and Moving Boundary and Diffusion Problems (Canberra, 1990)*. Canberra: Austral. Nat. Univ. Canberra (1992) pp. 154—176.
3. J. R. Cannon, R. B. Guenther and F. A. Mohamed, On the rainfall infiltration through a soil medium. *SIAM J. Appl. Math.* 49 (1989) 720–729.
4. J.-Y. Parlange, Theory of water movement in soils: 8 one-dimensional infiltration with constant flux at the surface. *Soil Science* 114 (1972) 1–4.
5. J. R. Philip, Theory of infiltration. *Advances in Hydroscience* 5 (1969) 215–292.
6. L. A. Richards, Capillary conduction of liquids through porous mediums. *Physics* 1 (1931) 318–333.
7. C. N. Dawson, C. J. van Duijn and R. E. Grundy, Large time asymptotics in contaminant transport in porous media. *SIAM J. Appl. Math.* 56 (1996) 965–993.
8. R. E. Grundy, Asymptotic solution of a model nonlinear convective diffusion equation. *IMA J. Appl. Math.* 31 (1983) 121–137.
9. C. J. van Duyn and J. M. de Graaf, Limiting profiles in contaminant transport through porous media. *SIAM J. Math. Anal.* 18 (1987) 728–743.
10. G. Fennemore and J. X. Xin, Wetting fronts in one-dimensional periodically layered soils. *SIAM J. Appl. Math.* 58 (1998) 387–427.
11. C. Cuesta, C. J. van Duijn and J. Hulshof, Infiltration in porous media with dynamic capillary pressure: travelling waves. *European J. Appl. Math.* 11 (2000) 381–397.
12. I. Mitkov, D. M. Tartakovsky and C. L. Winter, Dynamics of wetting fronts in porous media. *Phys. Rev. E* 58 (1998) 5245–5248.
13. R. E. Ewing and H. Wang, A summary of numerical methods for time-dependent advection-dominated partial differential equations. *J. Comp. Appl. Math.* 128 (2001) 423–445.
14. P. L. Sachdev, *Nonlinear Diffusive Waves*. Cambridge: Cambridge University Press (1987) 246 pp.
15. K. T. Joseph and P. L. Sachdev, Exact analysis of Burgers equation on semiline with flux condition at the origin. *Int. J. Non-Lin. Mech.* 28 (1993) 627–639.
16. V. Vanaja and P. L. Sachdev, Asymptotic solutions of a generalized Burgers equation. *Quart. Appl. Math.* 50 (1992) 627–640.
17. J. Buckmaster, Viscous sheets advancing over dry beds. *J. Fluid Mech.* 81 (1977) 735–756.
18. D. G. Aronson, Regularity of flows in porous media: a survey. In: W.-M. Ni, L. A. Peletier and J. Serrin (eds.), *Nonlinear Diffusion Equations and Their Equilibrium States, I (Berkeley, CA, 1986)*. New York: Springer (1988) pp. 35–49.
19. L. A. Peletier, Asymptotic behavior of solutions of the porous media equation. *SIAM J. Appl. Math.* 21 (1971) 542–551.
20. G. I. Barenblatt, *Scaling, Self-Similarity, and Intermediate Asymptotics*. Cambridge: Cambridge University Press (1996) 386 pp.
21. W. L. Kath and D. S. Cohen, Waiting-time behavior in a nonlinear diffusion equation. *Stud. Appl. Math.* 67 (1982) 79–105.
22. J. R. King, Approximate solutions to a nonlinear diffusion equation. *J. Engrg. Math.* 22 (1988) 53–72.
23. T. P. Witelski, Stopping and merging problems for the porous media equation. *IMA J. Appl. Math.* 54 (1995) 227–243.
24. T. P. Witelski, Perturbation analysis for wetting fronts in Richards' equation. *Transp. Porous Media* 27 (1997) 121–134.

25. J. Kevorkian and J. D. Cole, *Multiple Scale and Singular Perturbation Methods*. New York: Springer-Verlag (1996) 632 pp.
26. A. T. Corey, *Mechanics of Immiscible Fluids in Porous Media*. Littelon, Colorado: Water Resources Publications (1986) 259 pp.
27. D. G. Aronson, The porous medium equation. In: A. Fasano and M. Primicerio (eds.), *Nonlinear Diffusion Problems (Montecatini Terme, 1985)*. Berlin: Springer-Verlag (1986) pp. 1–46.
28. B. H. Gilding, Qualitative mathematical analysis of the Richards equation. *Transp. Porous Media* 5 (1991) 651–666.
29. D. A. Barry, J.-Y. Parlange, G. C. Sander and M. Sivaplan, A class of exact solution for Richards' equation. *J. Hydrology* 142 (1993) 29–46.
30. J. R. Philip, The theory of infiltration: 1 the infiltration equation and its solution. *Soil Science* 83 (1957) 345–357.
31. J. R. Philip, The theory of infiltration: 2 the profile at infinity. *Soil Science* 83 (1957) 435–448.
32. P. J. Ross and J.-Y. Parlange, Investigation of a method for deriving unsaturated soil hydraulic properties from water content profiles. *Soil Science* 157 (1994) 335–340.
33. I-Dee Chang, Navier-Stokes solutions at large distances from a finite body. *J. Math. Mech.* 10 (1961) 811–876.
34. P. A. Lagerstrom, *Matched Asymptotic Expansions*. New York: Springer-Verlag (1988) 250 pp.
35. I. G. Lisle and J.-Y. Parlange, Analytical reduction for a concentration dependent diffusion problem. *ZAMP* 44 (1993) 85–118.
36. B. H. Gilding, On a class of similarity solutions of the porous media equation. III. *J. Math. Anal. Appl.* 77 (1980) 381–402.
37. S. Kamin, Some estimates for solution of the Cauchy problem for equations of a nonstationary filtration. *J. Differential Equations* 20 (1976) 321–335.
38. G. H. Pimbley Jr, Wave solutions travelling along quadratic paths for the equation $(\partial u/\partial t) - (k(u)u_x)_x = 0$. *Quart. Appl. Math.* 35 (1977) 129–138.
39. T. P. Witelski, Horizontal infiltration into wet soil. *Water Resources Res.* 34 (1998) 216–222.
40. J.-Y. Parlange, W. L. Hogarth, C. Fuentes, J. Sprintall, R. Haverkamp, D. Elrick, M. B. Parlange, R. D. Braddock and D. A. Lockington, Superposition principle for short-term solutions of Richards equation - application to the interaction of wetting fronts with an impervious surface. *Transp. Porous Media* 17 (1994) 239–247.
41. W. L. Hogarth, J.-Y. Parlange, J. Sprintall, R. Haverkamp and M. B. Parlange, Addendum to interaction of wetting fronts with an impervious surface. *Transp. Porous Media* 21 (1995) 95–99.
42. J.-Y. Parlange, W. L. Hogarth, C. Fuentes, J. Sprintall, R. Haverkamp, D. Elrick, M. B. Parlange, R. D. Braddock and D. A. Lockington, Interaction of wetting fronts with an impervious surface - longer time behavior. *Transp. Porous Media* 17 (1994) 249–256.